

SOME FUNDAMENTAL COMBUSTION PROPERTIES OF "CRYOGENIC" PREMIXED HYDROGEN AIR FLAMES

Proust, C.^{1,2}, Jamois, D.¹

¹ Institut National de l'Environnement Industriel et des RISques (INERIS), Parc Technologique ALATA, PO box 2, Verneuil-en-Halatte, 60550, France, christophe.proust@inersi.fr

² University de Technologie de Compiègne (UTC), Alliance Sorbonne Université, centre de recherche Pierre Guillaumat, Compiègne, 60200, France

ABSTRACT

Because of the emergence of the U.E. "green deal" and because of the significant implication of national and regional authorities throughout Europe, the "hydrogen" economy is emerging. And with it, numerous questions and experimentations. One of them, perhaps a key point, is the storage and transport of hydrogen. Liquid hydrogen in cryogenic conditions is a possibility already used in the space industry but under a lot of constraints. What may be acceptable in a well-controlled and restrained domain may not be realistic in a wider application, closer to the public. Safety should be ensured and there is a need for a better knowledge of the flammable and ignition properties of the "cold" hydrogen mixtures following a cryogenic spillage for instance to select adequate ATEX equipment. The purpose of PRESLHY project [4] is to investigate the ignition, fire and explosion characteristics of cryogenic hydrogen spillages and to propose safety engineering methods. The present work is part of it and addresses the measurement of the laminar burning velocity (SI), flammability limits (FL), minimum ignition energy (MIE)... of hydrogen air mixtures at atmospheric pressure but down to -150°C. To do this, a special burner was designed with details given inside this paper together with the experimental results. It is found that the FL domain is reduced when the temperature drops, that MIE increases slightly and SI decreases..

1.0 CONTEXT AND OBJECTIVES

It is clear for most of the stakeholders of the "hydrogen energy" economy that ensuring the safety of hydrogen objects is a major constraint [1]. Failing in doing so may seriously jeopardize future developments. Because of the specificities of hydrogen [2], many leakage scenarios may degenerate in escalating accidents [3] and the very details of each scenario need to be described, quantified before designing, calculating the mitigation barriers. Explosion risk is certainly the most important.

As recalled by Jordan et al. [4], transporting and utilizing hydrogen as a cryogenic liquid (LH₂) may be a viable solution especially when large quantities are required. Because of the lack of knowledge about many aspects of the consequences of a LH₂ leakage, the project PRESLHY was funded by E.U. Progresses of the project are regularly presented and details can be found on www.preslhy.eu.

The present work is part of PRESLHY and deals with the evolution of the very basic ignition and combustion parameters as function of the temperature and composition of a cloud following a LH₂ leakage. The laminar burning velocity (SI), the minimum ignition energy (MIE) and the flammability range (FL) were investigated.

To do this a special type of burner was devised. A new type of spark generator, more accurate, was produced and infrared imaging was used and qualified to derive SI. The burner, the spark generator and

the imaging systems are described in the first section. The experimental procedure and the results are presented in the second section.

2.0 EXPERIMENTAL SETUPS

In a former project [5] on LH₂ leakages, a correlation was established (Figure 1) between the local temperature and local concentration in the plume resulting from an atmospheric release of LH₂. A very similar correlation was found recently [6] within PRESLHY project suggesting the correlation is robust enough. It can be seen that the lowest temperature in the flammable zone reached at the upper flammability limit (70% H₂ v/v) is about 100 K so -170°C. This is the lowest temperature that we targeted to. The pressure is atmospheric.

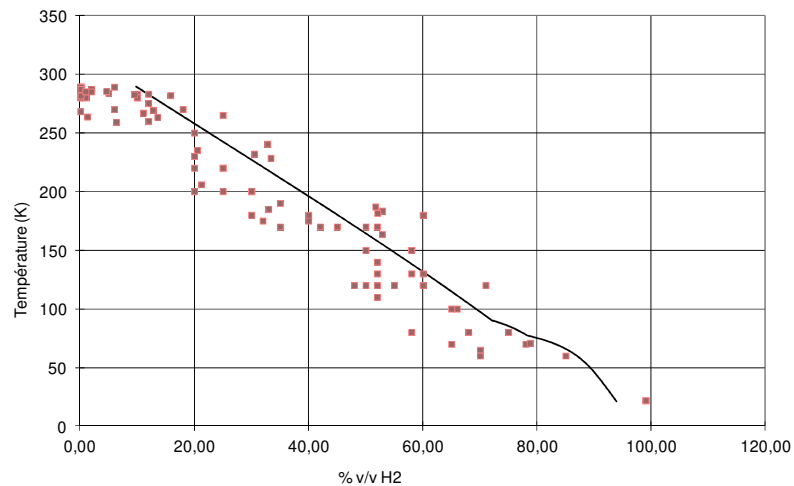


Figure 1: measurement of %H₂ and associated temperature in a plume resulting from an atmospheric release (free jet) of LH₂

A **special burner** was devised (Figure 2). It is a vertical metallic tube (40 mm diameter and about 400 mm high) filled with glass beads. Three 0.5 mm thermocouple (K type) are inserted into the bed: at the bottom, in the middle and at the top. The burner is thermally insulated using a special foam. The flammable mixture is introduced from the bottom and diffuses upwards. Ignition is produced just above the surface and the bed of particles quenches the flame. When cooled mixtures are desired, the bed is cooled before the tests by pouring about 2 liters of liquid nitrogen from the top. A typical temperature time curve is shown on Figure 3. There is time for about 30 mn of tests at reduced temperature.

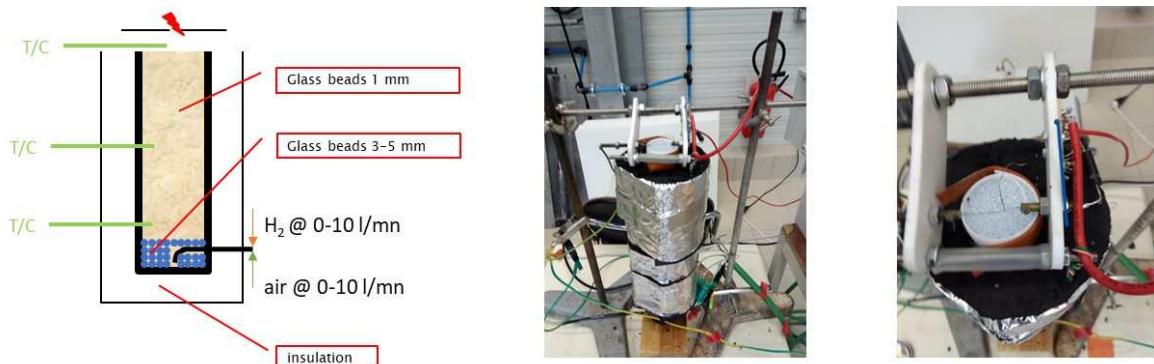


Figure 2: burner (40 mm ID and 400 mm high)

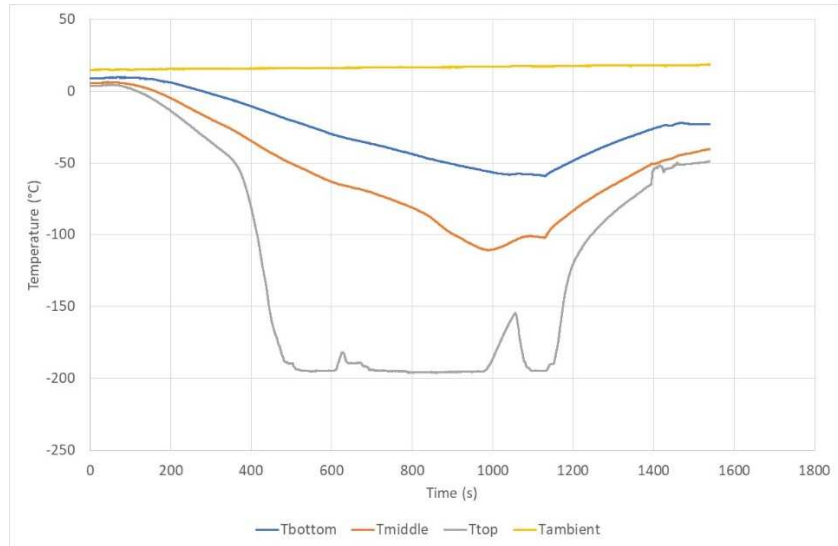


Figure 3: temperature evolution into the bed of glass beads after pouring 2 l of liquid nitrogen

Hydrogen and air are delivered from bottles. Air is “synthetic” containing 20.9% O₂ and the rest is N₂ with nearly no humidity (400 ppm). The mixture is prepared using calibrated mass flowmeters (Figure 4). Using a paramagnetic oxygen meter (SERVOMEX : O₂% accuracy = ±0.1% v/v) to control the mixture composition, it was checked that the ratio of the flowrates gives an accurate estimate of the real gaseous composition provided the mass flowmeters are operated between 10% and 90% of the full regulation range. It is believed that the absolute accuracy of the measurement of the concentration is ±0.5% v/v. It was further verified that the hydrogen concentration is constant over the cross section of the burner and up to some cms above.



Figure 4: mass flowmeter arrangement for hydrogen-air experiments (0-10 l/mn each)

To measure the minimum ignition energies or the flammability limits, the top of the burner was left fully open and the electrode system of the spark generator was placed very close to the top of the glass beads at a few mm from the top thermocouple (Figure 5). The flow velocity is on the order of 10 cm/s. To measure the burning velocities, higher velocities are necessary, at least double that of the laminar burning velocity. To achieve this a perforated cap was adjusted on the top of the burner. The orifice diameter is 4 mm with a profiled shape so that the discharge coefficient is about 0.85.

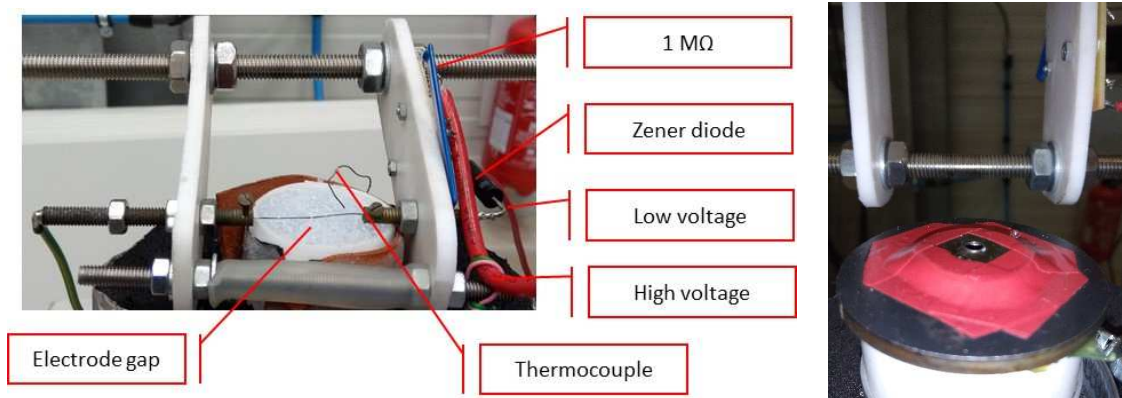


Figure 5: top burner arrangement (left : for MIE and PF; right : for SI)

A new type of **spark generator** was devised. It is designed to reduce the overlap between ignition and no ignition zones and to better control the energy delivered inside the spark gap. Details are given elsewhere [7]. An electrical spark is a two steps process. During the “disruption phase”, a large voltage is required (typically 3000 V/mm) to ionize the atmosphere and create a “streamer”. The current remains very low during that phase (micro amperes). After, the “arc” starts during which a large current flow through the spark gap. During this second phase, the voltage amounts some tens of volts with currents amounting some Amperes. In the present spark generator, it was decided to disconnect the two phases of the spark. A separate high voltage and high impedance circuit is used to produce the streamer (Figure 6). A second, low voltage and low impedance circuit, is used to produce the arc and dissipate the energy. The high voltage current is delivered through a set of 7 resistors (1 G Ω each) limiting the current supplied by the generator to about 1 μ A. The low voltage current is delivered to the charge capacitor through a set of 11 resistors (1 M Ω each) offering the possibly to produce continuous sparking at a rate of about 10-100 Hz. A 1 mH coil is in series to limit the current through the spark (thus decreasing Joule losses). A Zener diode prevents the high voltage to be transmitted to the low voltage circuit. The contactor is on the high voltage circuit. Once the streamer is created the low voltage circuit discharges automatically. The current is measured using a standard current gauge (torous) and the voltage with a high voltage probe. The electrodes are in tungsten, 0.3 mm in diameter, with gap of 0.5 mm.

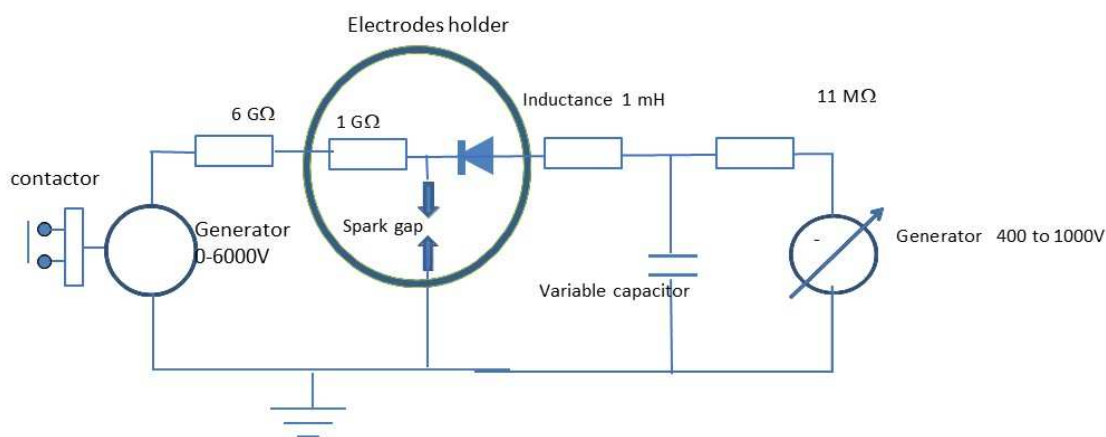


Figure 6: scheme of the electrical circuit

The spark gap and the Zener diodes being short circuited, the total capacitance of the low voltage part of the circuit is that of the charge capacitor. A residual value of 5-10 pF is constituted by the high voltage probe. If no coil is added, the inductance is 1.7 μ H and the resistance is 0.1 Ω . With the coil inserted, the inductance is 1 mH and the resistance is 2 Ω . Because of the high voltage required to trigger the arc, any capacitance on the high voltage side of the circuit may store and add a significant amount of energy to the spark under the form of a tiny precursor spark. It was measured that a 1 m high voltage

cable amounts about 20 pF which is much too large (energy stored = 90 μ J...). To remove this difficulty an extra resistor is added at the closest to the spark gap, on the electrode holder (Figure 5 left). Observations revealed that very tiny sparks occurred even when the low voltage circuit was not charged (Figure 7). This means that a residual capacitance remained. The high voltage circuit and the Zener diode are responsible for this. It was found that the residual capacitance of the high voltage circuit is only 1 pF and that of the diode is 3 pF so, 4 pF in total. The breakdown voltage for the 0.5 mm gap in the air of the laboratory was about 3000 V. It was verified that these precursor sparks are not able to ignite any hydrogen air mixtures. The energy delivered by the precursor spark was added up to that of the low voltage capacitance as shown later.

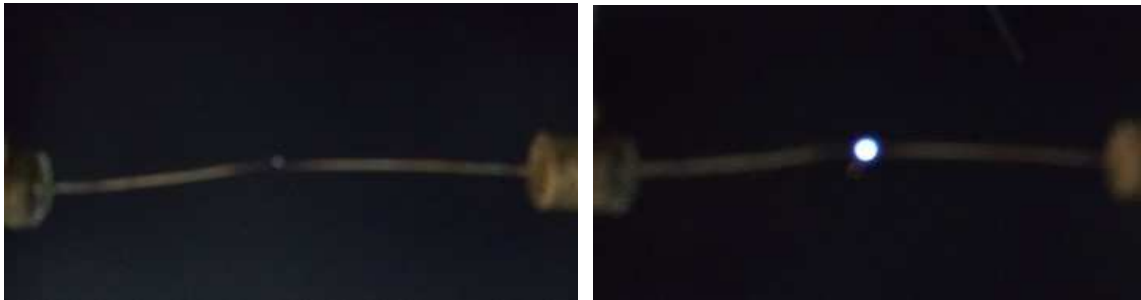


Figure 7: high voltage spark alone (left) and low voltage spark (right)

During the experimental campaign, the high voltage value was hardly varied and fixed to 5000 V. Note that this high voltage is never reached at the gap since the breakdown occurs at 3000 V max.

Further testing was performed to investigate the low voltage part behavior. The current and the voltage were measured at the spark gap (Figure 8). The very beginning of the current signal is an artifact probably due to the Zener diodes closing the low voltage part of the circuit. The signals resemble that of a typical RLC circuit and can be modelled rather faithfully. Such modelling can be used to estimate the yield of the spark (ratio of the electrical energy consumed in the spark gap divided by that stored in the low voltage capacitor). In the situation of Figure 8, with a reduced current, the yield is about 90%.

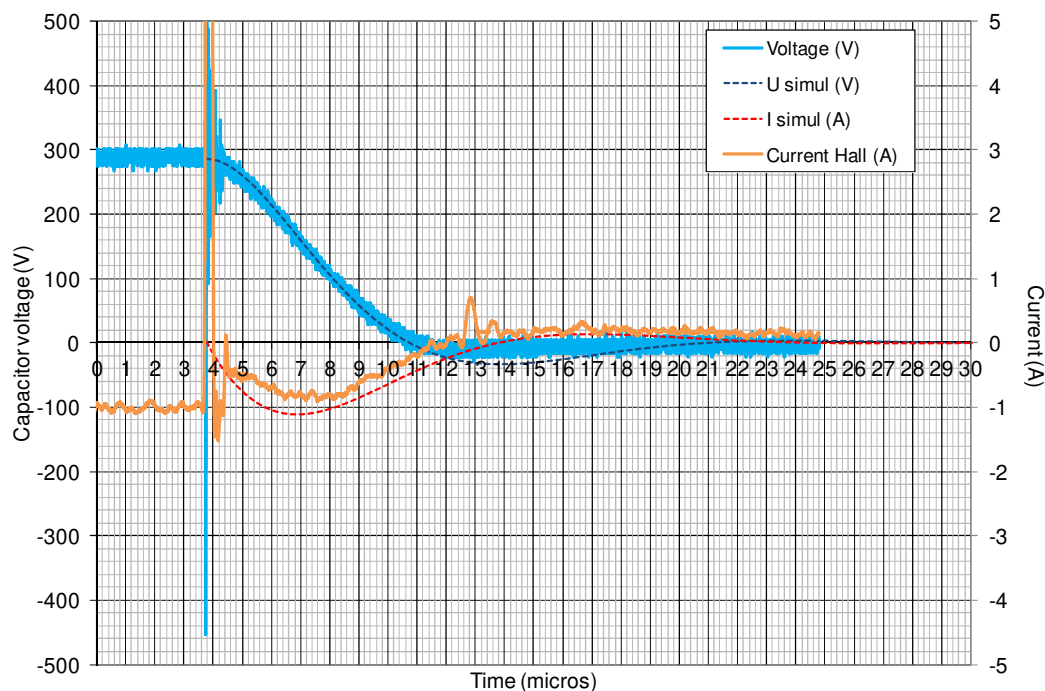


Figure 8: current voltage signals: streamer triggered spark, with a 1 mH additional inductance, 290 V in the 20 nF capacitor, with the diodes.

To measure the **laminar burning velocity**, the burner was equipped with the profiled orifice to increase the flow velocity. Then the “burner method” was used. The latter method [8, 9] has been used for a very long time and has been considerably refined. It is a reference method. With the burner arrangement proposed, the bed of glass beads is left 1 cm below the orifice. Since the orifice plate is very thin, it is believed that a top hat flow is produced [8]. The flame front is then a cone with straight slopes. The laminar burning velocity corresponds at best with the definition on the straight slope only. If α is the angle of the slope with the axis of the flow, the continuity equation at the flame front tells that:

$$Sl = U \cdot \sin \alpha$$

Where U is the flow velocity linked to the volumetric flowrate Q_v , orifice size (D_{burner}) and discharge coefficient Cd as:

$$U = \frac{Q_v}{Cd \cdot \frac{\pi}{4} \cdot D_{burner}^2}$$

But laminar hydrogen air flames are totally transparent and a simple, flexible and fast enough means to distinguish the flame front had to be designed. Since only little time is available for the measurements at very low temperatures (not more than a few minutes). Infrared video was used to do so. A FLIR A40 camera was used (50 fps; 256x256 pixels). Each test was filmed for a few seconds. The images of a sequence were converted into a grey scale and were summed up to increase the contrast. A typical example is shown on Figure 9-left. The aspect of the flame seems acceptable, but it is known that significant errors may come up if the position of the flame front is not accurately detected. To verify this, a shadowgraph of the same flame was done using a rough setup consisting in a standard video camera, a concave mirror and a led panel (Figure 10). The result is presented on Figure 9-right. Flame fronts are very similar suggesting the infrared technique can be used.

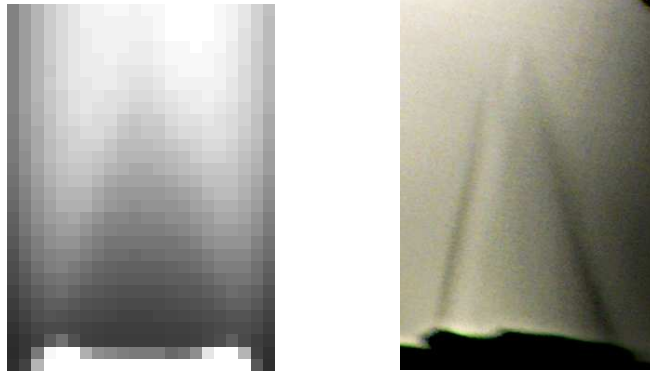


Figure 9: flame front for a 29% H₂ @20°C air mixture (left: from infrared video; right: shadowgraph)

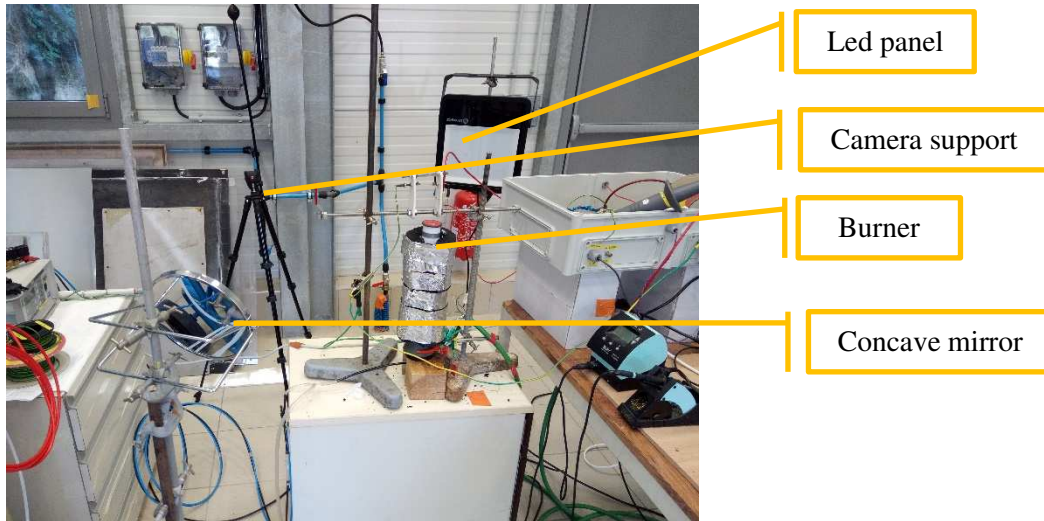


Figure 10: shadowgraph setup

3.0 RESULTS

First the **MIE measurement** method was designed and checked at ambient temperature. As experimentalists performing routinely such measurements know, the ignition threshold may differ when starting from the no ignition zone and increasing gradually the spark energy until ignition than when starting from a positive ignition point and decreasing the energy. MIEs are much higher with the former procedure. The reason is unclear but perhaps the combustion “cleans up” or chemically activates the tip of the electrodes. In the following, the ignition threshold at a given H_2 concentration was looked for using the second procedure (starting for a positive ignition and decreasing the energy). To vary the ignition energy, the value of the capacitor was adapted (100 pF to 5000 pF) and the voltage was varied (between 400 and 1000 V). The energies on the following graphs are that stored in the low voltage capacitor and in the streamer high voltage capacitors (4 pF). To calculate the latter the breakdown voltage was measured by decreasing the high voltage until no spark occurred anymore (2700 V with the air of the bottle at ambient temperature and atmospheric pressure). This voltage was used to calculate the energy coming from the high voltage side. No spark yield was introduced (yield=1) to be in conformity with the data from the literature.

Results obtained at room temperature are presented on figure 11. Note that each point represents at least 1 second of continuous sparking, so typically 50 sparks. The values are in line with the data from the literature [10] with a minimum at 20% amounting 18 μJ . There is little overlap between the no ignition zone and the ignition zone (a factor 2) which is much better than in previous studies (with a decade overlapping [11]). This shows that the ignition process is more deterministic than usually claimed. The present authors think the accuracy might be further improved.

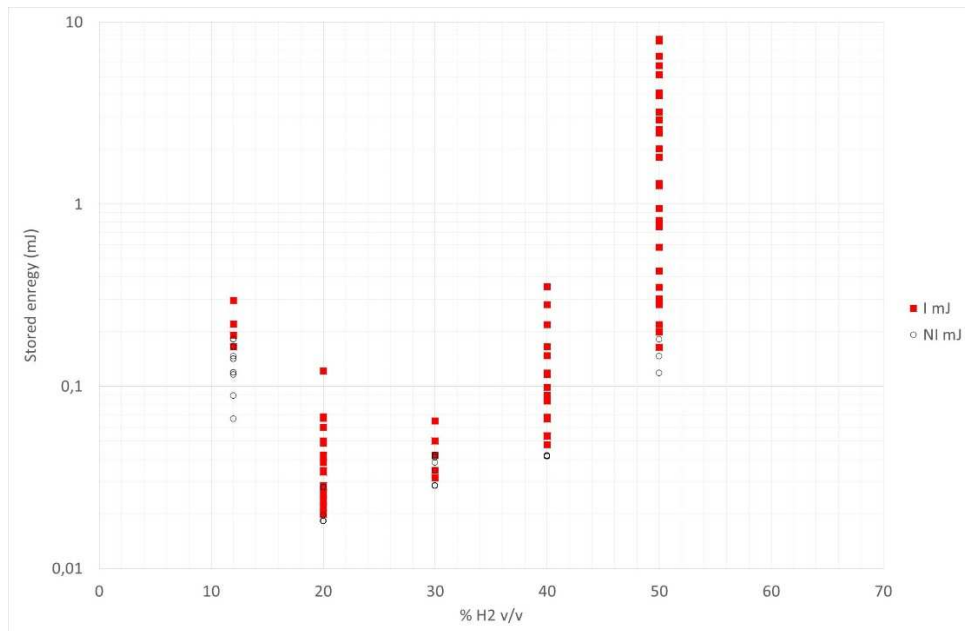


Figure 11: MIE for hydrogen-air mixtures at ambient temperature and atmospheric pressure (I means “ignition”, NI “no ignition”)

To estimate the amount of energy delivered by the high voltage spark, the breakdown voltage had to be measured (Figure 12). This was done for each test series. Although a great care was taken to control the distance between the electrodes (which should affect directly this voltage) some scattering is observed. This might come from the thermal dilatation of the electrodes which could change the distance between the tips but also from the status of the electrode tip. The location of the spark might not be the shortest geometrical path between the electrode tips. Globally the breakdown voltage increases when the temperature drops.

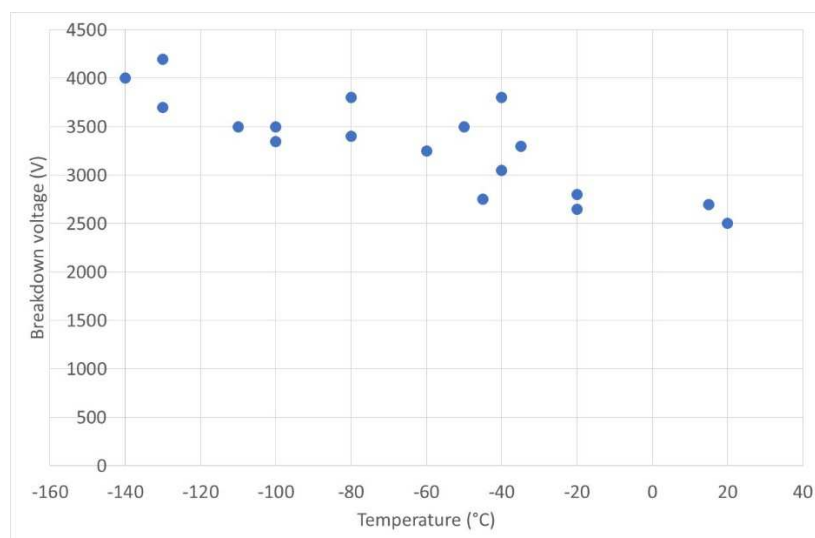


Figure 12: breakdown voltage as function of the temperature (pure air from the bottle)

MIE measurements were done at 20% and 30 % H₂ in air for temperatures ranging from -150°C to ambient (Figure 13). There is a slight but clear increase of MIE as the temperature drops.

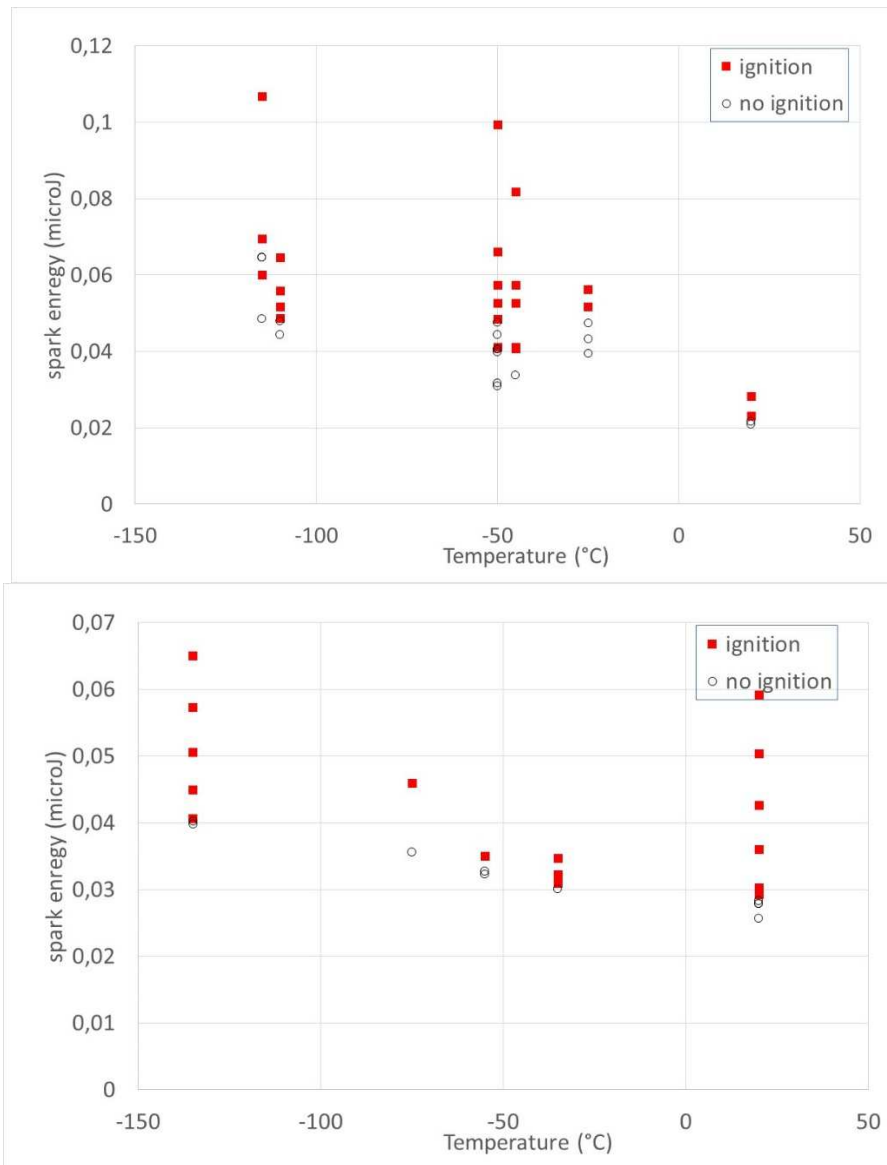


Figure 13: MIE of H₂-air mixtures as function of the temperature at atmospheric pressure (top : 20%; bottom : 30%)

To find out the **flammability limits** the same experimental arrangement was used but a much larger capacitor was used. A very large energy of 20 mJ was produced (64 nF under 800 V) which was judged enough according to the literature. The flame cannot be seen by eye and the ignition process is silent. To detect the flame the infrared camera (FLIR) was used. The results are presented in table 1. The flammability range decreases when the temperature drops, especially the upper flammability limit (UFL, LFL stands for “Lower Flammability Limit”).

Table 1 : LIE/LSE of H₂-air mixtures as function of the temperature at atmospheric pressure

Temperature (°C)	LFL (% H ₂ v/v)	UFL (% H ₂ v/v)
20	5	70
-60	5.6	66
-120	6	60

The laminar burning velocity measurements are shown of Figure 14. At ambient temperature, the measured laminar burning velocities are in line with other measurements [9]. Measurements at higher temperatures are available from Liu and Mc Farlane [12].

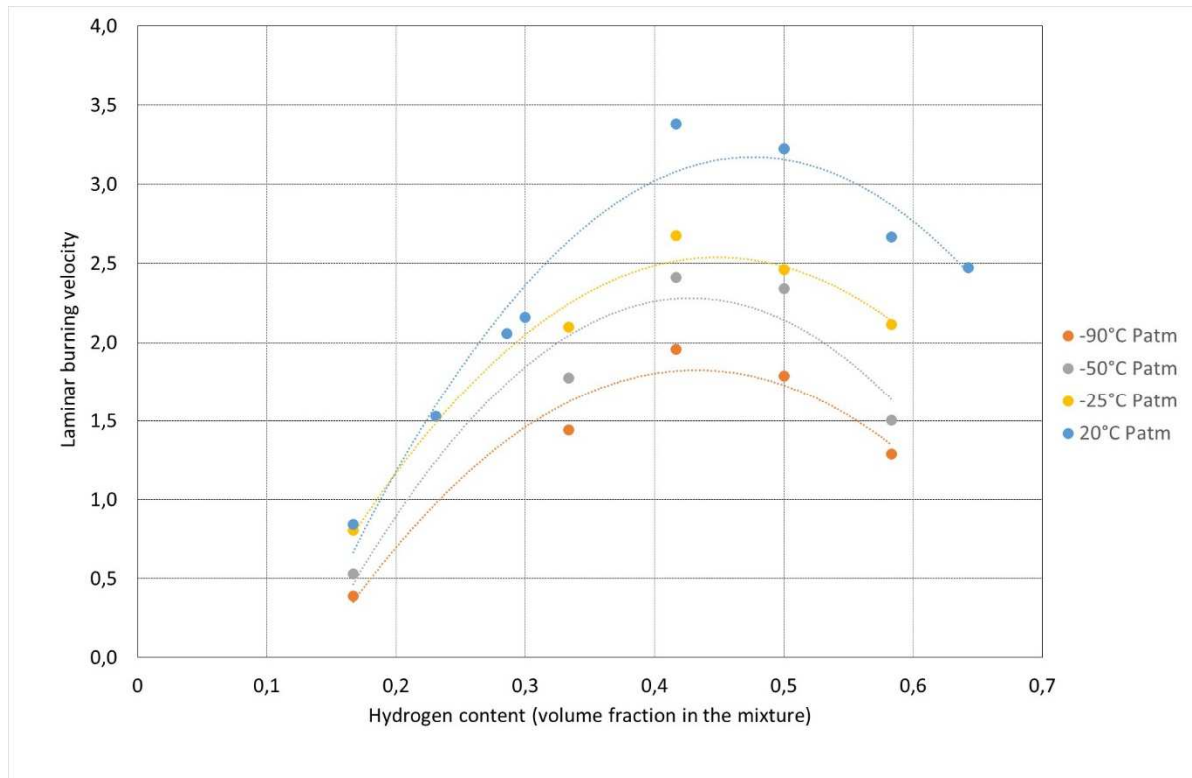


Figure 14: evolution of the laminar burning velocity as function of the temperature and of the mixture composition

To complete this investigation, the **expansion ratio** was calculated using a thermodynamic equilibrium code working at CEA [13]. The code minimizes the Gibbs energy of the products while conserving the enthalpy of the mixture (adiabatic combustion at constant pressure). The perfect gas law was used, and the chosen final combustion products are H_2O , OH , O , N , H , NO , O_2 , N_2 , H_2 . The simulations are done on the basis of 1 kg of mixture. The expansion ratio is the ratio between the volumes of the mixture before the combustion and after. Note that it is different from the ratio of the temperatures because of the variations of the change in the number of moles. The results are presented on figure 15.

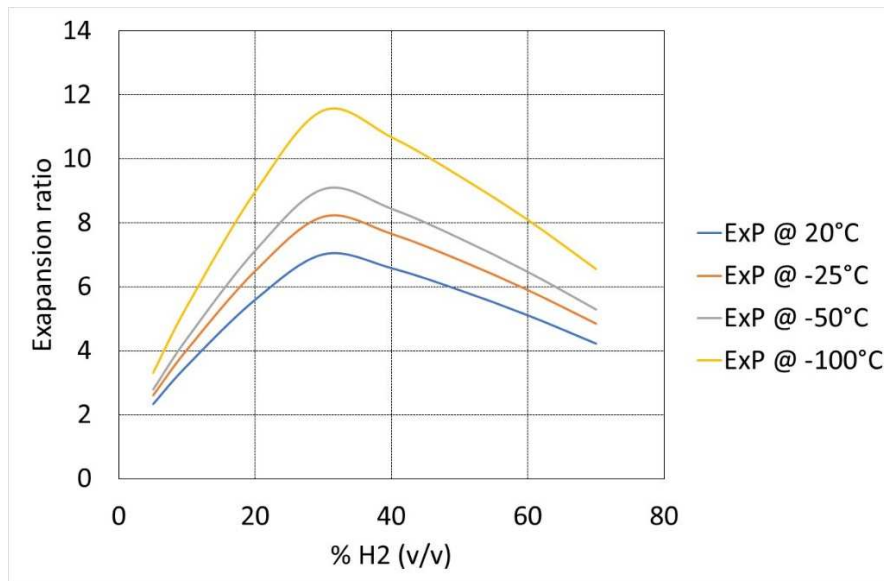


Figure 15: evolution of the expansion ratio of the combustion as function of the temperature and of the mixture composition

4.0 CONCLUSIONS

In this paper, a new experimental methodology to produce hydrogen-air mixtures at cryogenic temperatures is described. Experiments could be performed down to -150°C (atmospheric pressure) using a refrigerated burner. This burner can be used to measure most of the fundamental combustion parameters of such mixtures : minimum ignition energies (MIEs), flammability limits, laminar burning velocities.

A considerable effort was devoted to the measurement of MIEs. Because only a small influence of the temperature was expected, an accurate control of the spark and of the ignition was required. To that purpose a new spark generator was designed. Although some uncertainty remains, the ignition and no ignition zone overlap is very significantly reduced as compared to other equipment. Nevertheless, some variability remains probably due to the electrodes.

An alternative way (to schlieren) to detect the location of the flame front is proposed based on infrared imaging.

When decreasing the temperature, the minimum ignition energy (at 20% H₂) increases slightly from about 20 μJ at 20°C , to 40 μJ at -50°C and 50 μJ at -120°C . This is coherent with the decrease of the burning velocity with the temperature.

5.0 ACKNOWLEDGEMENT

The PRESLHY acknowledges the support granted by the European Fuel Cell and Hydrogen Joint Undertaking [FCH JU](#) under the Project ID 779613. The INERIS work programme acknowledges funding from the French ministry for Environment.

6.0 LITERATURE

1. Edwards, P. P.; Kutnetsov, V. L.; David, W. I. F., Hydrogen Energy , *Phil. Trans. R. Soc. A*, **365**, 2007, pp. 1043–1056
2. Crowl, D.A., Jo, Y.D., The hazards and risks of hydrogen, *Journal of Loss Prevention in the Process Industries*, **20**, 2007, pp. 158–164
3. Galassi, M.C., Papanikolaou, E., Baraldi, D., Funnemark, E., Håland, E., Engebø, A., Haugom, G.P., Jordan, J., HIAD – hydrogen incident and accident database, *International Journal of Hydrogen Energy*, **37**, 2012, pp. 17351–17357
4. Jordan, T.; Jallais, S.; Bernard, L.; Venetsanos, A.; Coldrick, S.; Kuznetsov, M.; Cirrone, D., Status of the Pre-Normative Research Project PRESLHY for the Safe Use of Liquid Hydrogen, *8th International Conference on Hydrogen Safety (ICHS 2019), Adelaide, Australia, 24.09.2019 – 26.09.2019*
5. Proust C., Chelhaoui S., Joly C., Processes of the formation and explosion of hydrogen-air clouds following an extensive spillage of liquid hydrogen, *National Hydrogen Association 12th Annual U.S. Hydrogen Meeting and Exposition, 2001*
6. Buttner, W.; Hall, J.; Coldrick, S.; Hooker, P.; Wishmeyer, T., Hydrogen wide area monitoring of LH2 releases, *International Journal of Hydrogen Energy*, **46**, 2021, pp. 12497–12510
7. Proust, C., A new technique to produce well controlled electrical sparks. Application to MIE measurements, *13th International Symposium on Hazards, Prevention, and Mitigation of Industrial Explosions, Braunschweig, GERMANY – July 27-31, 2020*
8. Bouvet, N.; Chauveau, C.; Gökalp I.; Lee, S.Y.; Santoro, R.J., Characterization of syngas laminar flames using the Bunsen burner configuration, *International Journal of Hydrogen Energy*, **36**, 2011, pp. 992-1005
9. Pareja, J.; Burbano, H.J.; Ogami, Y., Measurements of the laminar burning velocity of hydrogen–air premixed flames, *International Journal of Hydrogen Energy*, **35**, 2010, pp. 1812-1818
10. Ono, R.; Nifuku, M.; Fujiwara, S.; Horiguchi, S.; Oda, T., Minimum ignition energy of hydrogen–air mixture: Effects of humidity and spark duration, *Journal of Electrostatics*, **65**, 2007, pp. 87-93.
11. Eckhoff, R.K.; Ngo, M.; Olsen, W. , On the minimum ignition energy (MIE) for propane/air, *Journal of Hazardous Materials*, **175**, pp. 293–29
12. Liu, D.D.S.; Mc Farlane, R., Laminar burning velocities of hydrogen-air and hydrogen-air-steam flames, *Combustion and Flame*, **49**, 1983, pp. 59-71
13. Gordon, S.; McBride, B. J., Computer program for calculation of complex chemical equilibrium compositions and applications, Part 1: Analysis, 1994, *NASA reference publication 1311*.